# Hydraulic conductivity behavior of Gellan gum – treated sands considering stress variations in laboratory scale

Thi-Phuong-An Tran\*1, Ilhan Chang\*2, Minhyeong Lee3a, Gye-Chun Cho4b and Tran Thanh Nhan1c

<sup>1</sup>Department of Hydrogeological and Geotechnical Engineering, University of Sciences, Hue University, 77 Nguyen Hue, Vietnam <sup>2</sup>Department of Civil Systems Engineering, Ajou University, Suwon 16499, Korea <sup>3</sup>Disposal Performance Demonstration Research Division, Korea Atomic Energy Research Institute (KAERI), Daejeon 34057, Republic of Korea <sup>4</sup>Department of Civil Engineering, Korean Advanced Institute for Science and Technology, 291 Daehak-ro, Yuseong-gu, Daejeon 305-701, Republic of Korea

(Received February 5, 2024, Revised August 2, 2025, Accepted August 5, 2025)

**Abstract.** Biopolymer-based soil treatment (BPST) has recently been introduced as a new ground improvement method for environmentally friendly and sustainable development. Numbers of research have investigated BPST effects on the soil hydraulic conductivity, while there are lack of studies considering in-situ stress (i.e. vertical confinement and groundwater pressure) conditions. In this study, the effect of gellan gum BPST on the hydraulic conductivity behavior of sands was assessed using a pressurized permeability test apparatus which allows separate vertical confinement and pore pressure control. The hydraulic conductivity of gellan gum biopolymer-treated sands were measured with different biopolymer contents, vertical confinement levels, and pore water pressure conditions. Laboratory test results show that the hydraulic conductivity of gellan gum-treated sands attribute to 1) biopolymer-particle bonding, 2) biopolymer hydrogel induced pore-clogging, and 3) hydrogel alteration due to pore pressure increase, where gellan gum BPST is postulated to be an effective manner for ground hydraulic conductivity control in geotechnical engineering practice.

Keywords: effective stress; gellan gum; hydraulic conductivity; pore-clogging; water pressure

### 1. Introduction

Recently, interest in the use of biopolymer-based soil treatment (BPST) in geotechnical engineering has been rising over the last decade. Several studies have attempted to explain the effectiveness in soil strengthening (Chang and Cho 2019, Qureshi *et al.* 2022), soil hydraulic conductivity control (Chang *et al.* 2016), erosion reduction (Kwon *et al.* 2020, Shabani *et al.* 2022), dust control (Chang *et al.* 2020), heavy metal removal (Tran *et al.* 2021) and water retention (Chang *et al.* 2023, Tran *et al.* 2019) with BPST.

Biopolymer hydrogels are hydrophilic polymers which can absorb and retain water or biological fluids with structural stability (Guilherme *et al.* 2015). The hydrogel hydrophilicity attribute to the number of water–solubilizing groups (e.g., -OH, -COOH, -COO-, >C=O, >CHNH2, -CONH2, -SO3H) in the polymer network (Gun'ko *et al.* 2017). Previous studies show that the presence of hydrogel in the soil will affect the pore fluid viscosity and flow

bonding can physically improve the soil such as soil aggregate stabilization (Zhang *et al.* 2022), while hydrogel also effectively controls the soil hydraulic conductivity via pore-clogging (Chang *et al.* 2016). In addition, hydrogels can maintain higher soil moisture content which provides a proper effect on vegetation growth and survivability (Tran *et al.* 2019).

As the presence and flow of water in soil becomes an

behavior of clays (Chang *et al.* 1992, Heller and Keren 2002). Furthermore, hydrogel induced particle linkage or

important design consideration in geotechnical engineering, several studies have been attempted to investigate the effectiveness of hydrogels on soil hydraulic conductivity control (Chang et al. 2016, Tran et al. 2021). The interaction between a hydrogel and water molecular, which decides the viscosity and rheology behavior of the hydrogel (Dumitriu and Popa 2013), plays an important role to the hydraulic conductivity of soils (Kim and Corapcioglu 2002) at where the hydrogel is adapted. To investigate the poreclogging effect of hydrogels and hydrogel treatment to soils, recent studies mostly attempted two different approaches. The first is flowing deionized water through hydrogel-mixed soil using falling head permeability test (Andry et al. 2009), constant head permeameter (Narjary et al. 2012), and flexible wall permeameter (Chang et al. 2016) methods, while the other approach is using hydrogel solution itself as the main fluid to flow through soil medium (Etemadi et al. 2003). In this study, a pressured hydraulic conductivity apparatus which can represent ground stress

ISSN: 2005-307X (Print), 2092-6219 (Online)

<sup>\*</sup>Corresponding author, Ph.D.

E-mail: ttphuongan@hueuni.edu.vn

<sup>\*\*</sup>Corresponding author, Professor

E-mail: ilhanchang@ajou.ac.kr

aPh.D.

 $<sup>{}^{\</sup>rm b}$ Professor

<sup>&</sup>lt;sup>c</sup>Associate Professor

conditions (i.e., vertical confining stress and hydrostatic groundwater pressure) is introduced. Deionized water is used to be the main flowing fluid; thus, the test method suggested in this study can be regarded as an improved method for the first approach afore-mentioned.

This study aims to investigate the following phenomena: 1) the effect gellan gum BPST on the hydraulic conductivity behavior of sand and sand-clay mixture; 2) hydraulic conductivity behavior of gellan gum BPST considering insitu stress (vertical confinement and groundwater pressure) of laboratory conditions, through series hydraulic conductivity tests using pressurized hydraulic a conductivity test apparatus.

#### 2. Materials and experimental process

#### 2.1 Materials

#### 2.1.1 Soils

Jumunjin sand is a standard sand material in Korea which is classified as poorly graded sand (SP) according to the unified soil classification system (USCS). Jumunjin sand used in this study has an average particle size ( $D_{50}$ ) of 0.46 mm, specific gravity ( $G_s$ ) of 2.65, coefficient of uniformity ( $C_u$ ) and coefficient of curvature ( $C_c$ ) of 1.39 and 0.76, respectively (Chang and Cho 2019).

Clean sand and clay were dried in an oven at 105°C before specimen preparation. A sand-clay mixture (*SW-SM*) was represented by mixing sand and clay at the mass ratio of 9:1 (S9K1).

#### 2.1.2 Gellan gum

Gellan gum (hereinafter, GG) is a linear polysaccharide produced by Pseudomonas elodea bacterium, and mainly consists repeating tetrasaccharide (D-glucose(β1→4), Dglucuronate( $\beta 1 \rightarrow 4$ ), D-glucose( $\beta 1 \rightarrow 4$ ), rhamnose( $\alpha 1 \rightarrow 3$ ) (Milas et al. 1990). GG hydrogel shows temperature-dependent rheology where GG solubility with low viscosity at temperature above 90°C, while GG undergoes thermogelatin process when cooled below 40°C, a highly viscous hydrogel is formed. Thus, GG has been used as thickener and gelatin agents in biomedical applications (Osmałek et al. 2014), food products (Paul et al. 1986). In geotechnical engineering, GG has been introduced as a soil binder (Chang et al. 2020, Tran et al. 2023, Tran et al. 2022), especially for enhancing the wet (or saturated) strength of soils (Chang and Cho 2019). Low acyl GG biopolymer supplied by Sigma Aldrich (CAS no.71010-52-1) was used in this study.

## 2.1.3 Gellan gum biopolymer-based soil treatment

For the preparation of thermo-gelated GG biopolymertreated soil specimens, GG was dissolved and hydrated in deionized water heated at 100°C, resulting in a homogenous GG hydrogel solution. Dried soil and GG solution were then mixed using a laboratory motar mixer to ensure thorough bending. to prevent thermo-gelation during mixing, the process was conducted at temperature above 85°C according to Chang *et al.* (2015c). After mixing, the

Table 1 Specimens and experimental conditions

Soil types	Gellan gum content [%]	Initial water content [%]	Vertical confining stress, $\sigma_v$ [kPa]	Constant hydraulic pressure, <i>u</i> <sub>in</sub> [kPa]	
Sand (S10)	0, 0.50	30			
	1.00	36		70 ≤ Δu	
	2.00	44			
Sand 90%– kaolinite 10% (S9K1)	0, 0.25, 0.40, 0.50	30	100; 200;		
	0.75	35	400		
	1.00	36			
	1.50	38			
	2.00	44			

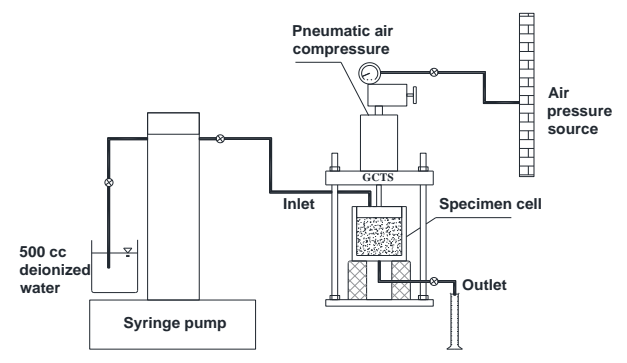


Fig. 1 Schematic diagram of pressurized hydraulic conductivity apparatus

GG-soil mixture was molded into the cylindrical specimen cell (80 mm in diameter, 93 mm in height) presented in Fig. 1. GG-soil mixture in the specimen cell was cooled down to room temperature (20°C) to complete the thermo-gelation process. Detail specimen conditions are summarized in Table 1.

### 2.2 Experimental procedure

#### 2.2.1 Experimental design and process

The saturated hydraulic conductivity of soils was assessed using a pressurized hydraulic conductivity test apparatus illustrated in Fig. 1. The initial height of specimens inside the cell was set at 70 mm. Filter papers were placed on the top and bottom of the specimen to allow water to evenly distribute and drain during the experimental program.

The vertical confining stress ( $\sigma_v$ ) was applied after 24 hours since the specimen was sufficiently cooled and thermo-gelated at room temperature. The  $\sigma_v$  was applied to the soil specimen under the drained condition using a pneumatic loader (GCTS FRM-10P), which was set at 100, 200, and 400 kPa (Table 1). The pre-compression was applied for 24 hours until no more vertical strain has been observed (Figs. 2(a) and 2(b)). The amount of water drainage from the soil specimen during pre-compression was less than 6% of the initial water content values listed in Table 1. The water drainage depended on the GG content

Gellan content [%		gum to soil mass $(m_b/m_s)$	0	0.25	0.40	0.50	0.75	1.00	1.50	2.00
S10 $\rho_d$	$ ho_d$	$[g/cm^3]$	1.48			1.66		1.48		1.50
	n	[%]	44.1			37.4		43.5		43.3
S9K1	$ ho_d$	[g/cm <sup>3</sup> ]	1.53	1.62	1.57	1.77	1.51	1.53	1.58	1.58
	n	[%]	42.3	39.1	40.7	33.1	41.4	42.5	40.6	41.1

Table 2 Dry density and porosity of GG-treated soils

 $(c_{gg})$ , where higher cgg renders less water drainage from the soil (e.g., for GG-treated S9K1 soil, water drainage compared to the initial water content were 6% and 1.3% for 0.25% and 2% cgg, respectively). The dry density and porosity of soil samples after pre-compression are summarized in Table 2.

After pre-compression, the pneumatic loader was set to maintain the applied  $\sigma_{\nu}$  level then water was supplied at the bottom using a syringe pump (Teledyne ISCO 500D) to saturate the soil sample in the specimen cell. The outlet valve on the top cap was opened for de-airing until an outlet water flow has been observed. Once water outflow has been observed, the valve on the top cap was connected to the syringe pump with the outlet valve on the cell bottom being closed. Water was pumped into the specimen until the hydraulic pressure reached and stabilized to the target hydraulic value (> 70 kPa), where this stage is regarded to be the pressurized saturated condition in this study. After specimen saturation, the outlet valve on the bottom was opened, and the hydraulic conductivity has been assessed under a constant hydraulic pressure (hereinafter,  $u_{in}$ ) condition controlled by the syringe pump device. The hydraulic conductivity measurement has been conducted for 24 hours.

#### 2.2.2 Analysis method

The soil porosity (*n*) of sand (S10) samples ranges 37.4 to 44.1% (Table 2), which is higher than a body-centered cube (n = 32.0%) but lower than a simple cube (n = 47.6%) structure. Thus, if considering a body-centered structure, the equivalent diameter of pore spaces ( $d_{eq}$ ) can be estimated as

$$V_{pore} = 0.32 \times V_{total} = 0.32 \times \left(\frac{4r}{\sqrt{3}}\right)^{3} = 0.32 \times \left(\frac{2D_{50}}{\sqrt{3}}\right)^{3}$$
$$= 0.49 (D_{50})^{3}$$
(1)

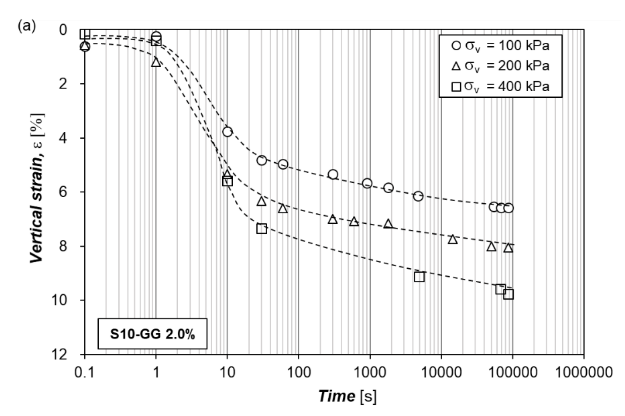
where  $V_{pore}$  is the pore volume,  $V_{total}$  is the total volume of cube soil and r is atomic radius of a soil particle

$$V_{pore} = \left(\frac{\pi \times d_{eq}^{2}}{4}\right) \times \text{ height of unit cell}$$

$$= \left(\frac{\pi \times d_{eq}^{2}}{4}\right) \times \left(\frac{4\sqrt{3}}{3} \frac{D_{50}}{2}\right)$$
(2)

As Eqs. (1) and (2),  $deq = 0.74 \times D50 = 0.34$  mm, where deq can be regarded as the minimum opening size of a flow path between sand particles;

Meanwhile, the overall equivalent diameter  $(D_{eq})$  of pore spaces of the entire specimen volume can be derived as



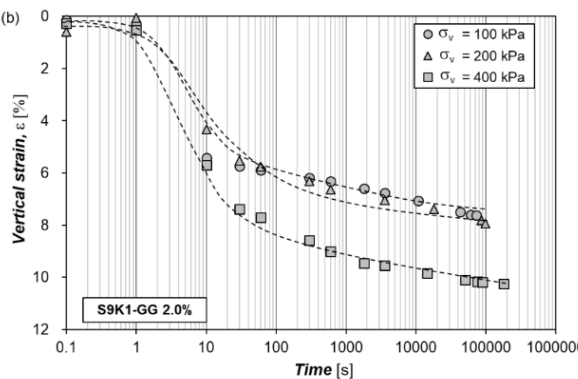


Fig. 2 Vertical deformation of 2% gellan gum biopolymer-treated (a) 100% sand (S10) and (b) sand–kaolinite mixture (S9K1) at different vertical confining stresses

$$D_{eq} = \sqrt{\frac{4V_{\nu}}{\pi H}} \tag{3}$$

where  $V_{\nu}$  is the void volume and H is the height of the specimen. Thus,  $D_{eq}$  becomes 0.05 m on average. Thus, the possible number of flow paths (N) in the soil system can be estimated as

$$N = \left(\frac{D_{eq}}{d_{eq}}\right)^2 = \left(\frac{50 \text{ mm}}{0.34 \text{ mm}}\right)^2 \approx 21626 \text{ paths}$$
 (4)

The Reynold's number (Re) for water flow through soil is known to be

$$R_e = \frac{\rho.v.D_{eq}}{u} \tag{5}$$

where  $\rho$  is water density (998 kg/m<sup>3</sup>),  $\nu$  is the flow velocity

Gellan	Vertical	<u> </u>	S10		<u>-</u>	S9K1	
content [%]	confining stress [kPa]	Constant hydraulic pressure			Constant hydraulic pressure		
		100	200	400	100	200	400
0	100	22.03	32.43	48.90	23.30	30.56	36.53
	400	21.65	22.11	38.67	22.74	27.68	37.06
0.25	100				0.85	1.65	
	400				0.08	0.18	1.01
0.4	100				0.054	0.101	
	400				0.032	0.052	0.395
0.5	100	1.21	0.87		0.02		
	400	0.45	0.85	2.86	0.01	0.01	0.01
0.75	100				< 0.01	< 0.01	
	400				0.02	0.01	0.01
1.0	100	0.02			0.01	0.02	
	400	0.01	0.04	0.22	0.01	< 0.01	0.01
1.5	100				0.01	0.03	
	400				0.01	0.01	0.01
2.0	100	0.04	0.09		< 0.01	0.03	
	400	< 0.01	< 0.01	0.12	< 0.01	0.01	< 0.02

Table 3 Reynolds number values calculated based on  $D_{eq}$ 

through flow paths (i.e.,  $Q_{out}/\left(\frac{\pi D_{eq}^2}{4}\right)$  m/s),  $Q_{out}$  is the volumetric outlet flow rate (m<sup>3</sup>/sec), and  $\mu$  is fluid viscosity (1 × 10<sup>-3</sup> kg/ms).

When  $R_e$  < 10, the flow through a porous medium is regarded as laminar flow (Bear 2012, 2013) while contrary ( $R_e > 10$ ) indicates transitional or turbulent flows (Chen & Wagenet 1992). The  $R_e$  values of soil specimens assessed in this study are summarized in Table 3, where the flow through untreated soil is classified as non-laminar flow due to the high  $Q_{out}$  (9.07 x  $10^{-7} \sim 2.05$  x  $10^{-6}$  m³/sec); thus, hydraulic conductivity (k) is calculated as follows (Mulqueen 2005).

$$k = \frac{Q_{out}}{A} \left(\frac{H}{\Lambda h}\right)^{0.5} \tag{6}$$

where H is the height of soil specimen, A is the cross-sectional area of soil specimen, and  $\Delta h$  is the head difference.

Meanwhile, the water flow through GG-treated soils are all classified as laminar flow conditions ( $R_e < 10$ , Table 3) due to the low  $Q_{out}$  (8.80 x  $10^{-11} \sim 1.10$  x  $10^{-7}$  m<sup>3</sup>/sec). Thus, the k for GG-treated soil can be evaluated using Darcy's law

$$k = \frac{Q_{out}}{A} \left(\frac{H}{\Delta h}\right) \tag{7}$$

The Reynolds number and hydraulic conductivity calculations used in the study are based on formulations that assume homogeneous and linear flow conditions.

#### 3. Results and analysis

3.1 Hydraulic conductivity of GG-treated soils with hydraulic pressure variation

Fig. 3 shows the measured k values of S10 soil with  $c_{gg}$ ,  $\sigma_v$ , and  $u_{in}$  variations. Untreated S10 (S10-GG 0%) showed almost constant k values in a range of 3.50  $\sim$  2.43  $\times$  10<sup>-5</sup> m/s, regardless of  $\sigma_v$  and  $u_{in}$  increases (Fig. 3(a)). As S10 is treated with GG, the k value at  $u_{in} = 70$  kPa reduced significantly in order of  $c_{gg}$  increase (Figs. 3(b)-3(d)). Thereafter, k gradually decreased to a minimum value ( $k_{min}$ ) and then turned to increase with  $u_{in}$  increase.

The k- $u_{in}$  relationship of S9K1 soil with different  $c_{gg}$  values are presented in Fig. 4. The k value at  $u_{in} = 70$  kPa generally decreased with  $c_{gg}$  increase up to 0.5% (Figs. 4(b)-4(d)), while higher (>0.5%)  $c_{gg}$  conditions did not render further k reduction (Figs. 4(e)-4(h)). Furthermore, for the untreated S9K1 (S9K1-GG 0%), the k values were in a range of 2.98  $\sim 2.28 \times 10^{-5}$  m/s (Fig. 4(a)), close to the k range of untreated S10 (Fig. 3(a)) which is regarded to be induced by the loss of kaolinite particles with the  $u_{in}$  relationship also starts decrease to a  $k_{min}$  followed by a gradual increase with  $u_{in}$  variation for  $c_{gg} > 0.4\%$  conditions (Figs. 4(c)-4(h)).

Fig. 6 shows how the  $k_{min}$  of the GG-treated soils were obtained in this study. Two tangent lines along the decline and increase paths were plotted, where the intersection marks  $k_{min}$  and the corresponding hydraulic pressure at  $k_{min}$  ( $P_{kmin}$ ). For instance, S9K1-GG 1.5% soil is assessed to have  $k_{min} = 4.69 \ 10^{-11}$  m/sec at  $P_{kmin} = 416$  kPa (Fig. 6). The relationship between  $k_{min}$ ,  $c_{gg}$ , and  $\sigma_v$  will be discussed in following sections.

# 3.2 Effect of GG content and vertical confining stress on the hydraulic conductivity behaviour

Fig. 7 presents the  $k_{min}$  variation of GG-treated sands with different  $c_{gg}$  and  $\sigma_v$  levels. The  $k_{min}$  of GG-treated S10

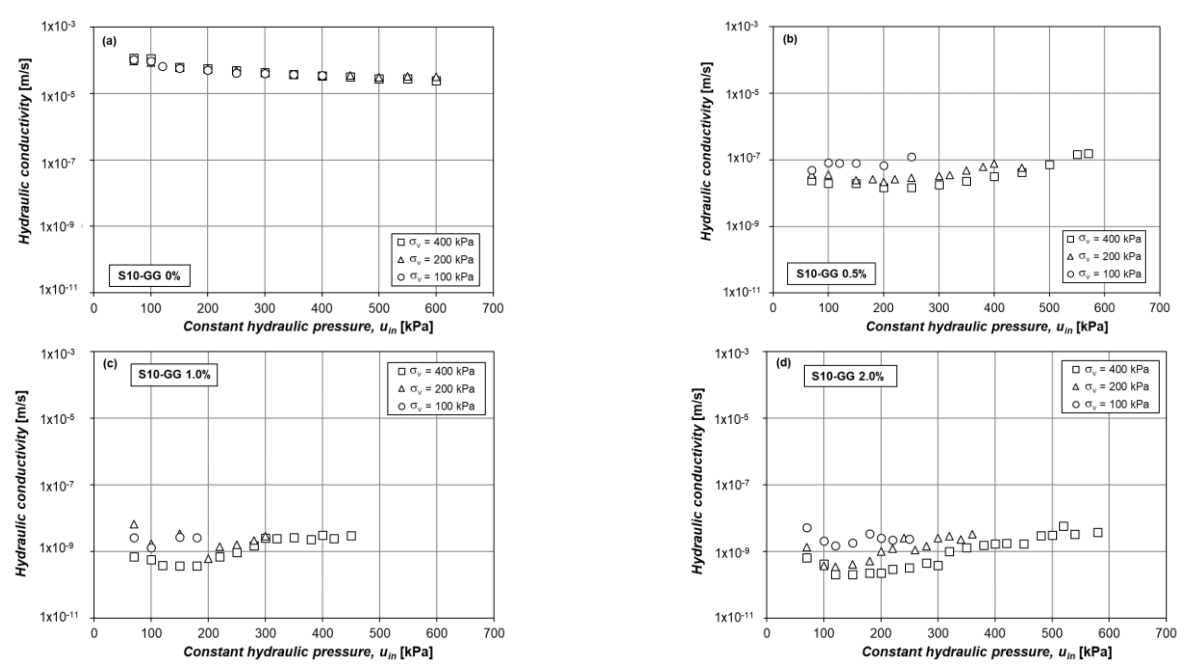


Fig. 3 Hydraulic conductivity with constant hydraulic pressure of sand (S10) with biopolymer-based soil treatment (a) 0.0%, (b) 0.5%, (c) 1.0 % and (d) 2.0% gellan gum

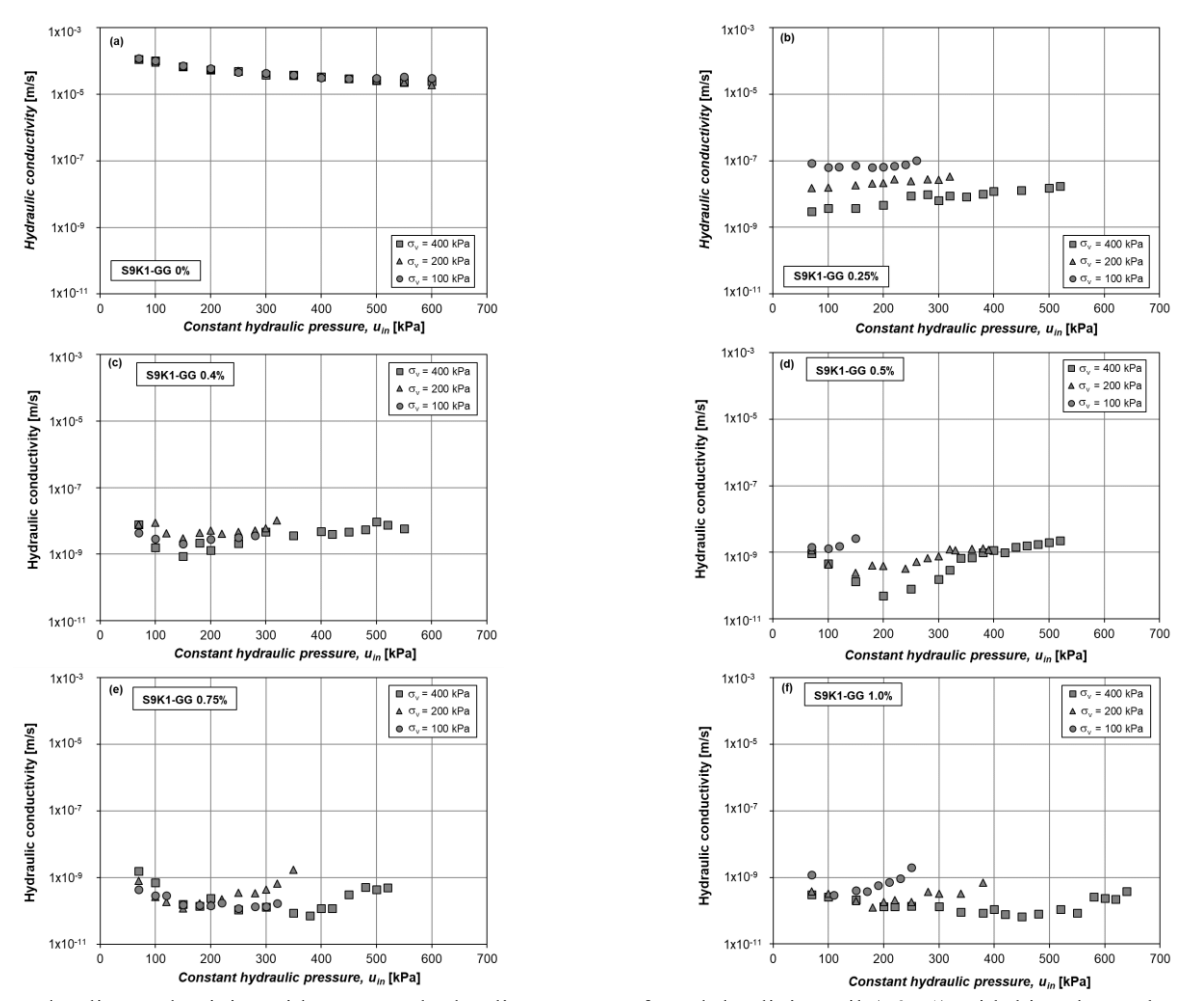
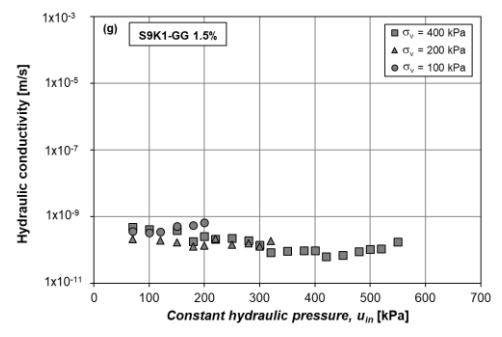


Fig. 4 Hydraulic conductivity with constant hydraulic pressure of sand–kaolinite soil (S9K1) with biopolymer-based soil treatment (a) 0.0%, (b) 0.25%, (c) 0.4%, (d) 0.5%, (e) 0.75%, (f) 1.0%, (g) 1.5% and (h) 2.0% gellan gum



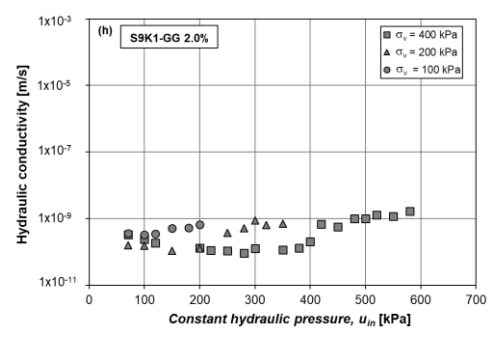


Fig. 4 Continued-

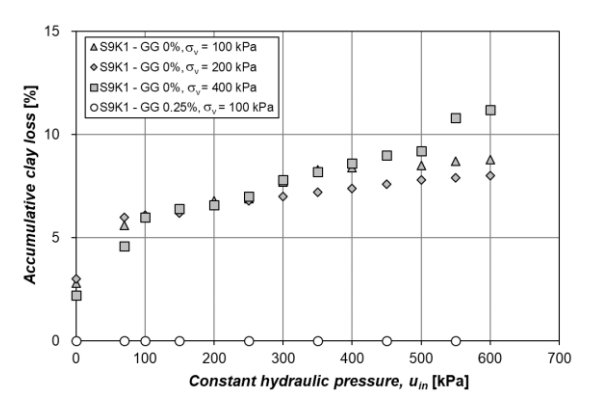


Fig. 5 The loss of kaolinite with the increase of constant hydraulic pressure

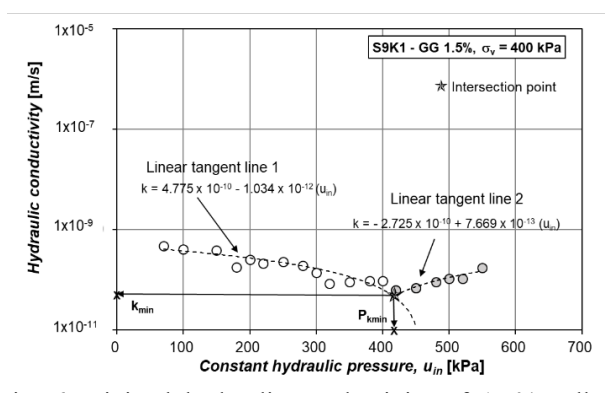


Fig. 6 Minimal hydraulic conductivity of 1.5% gellan gum-treated S9K1 soil under vertical confining stress of 400 kPa

significantly decreases with GG treatment and converges to a stable  $k_{min}$  value ( $k_{min} \le 1 \times 10^{-9}$  m/s) after  $c_{gg} \ge 1\%$  (Fig. 7(a)), which is in accordant to the findings by Chang *et al.* (2016) where higher  $c_{gg}$  values are expected to contribute more to hydrogel thickening and soil strengthening rather than pore-clogging (Chang *et al.* 2016).

S9K1 soil shows a steeper decline and starts to converge after  $c_{gg} \ge 0.5\%$  (Fig. 7(b)), where  $c_{gg} = 0.5\%$  for S9K1 soil is equivalent to 5% GG-to-kaolinite content in mass which is postulated to be the most optimal condition for GG-kaolinite matrix formation (Chang and Cho 2019). Results in Fig. 7(b) implies 5% GG-to-kaolinite content to be the most effective condition for not only soil strengthening (Chang and Cho 2019) but also for soil hydraulic conductivity control.

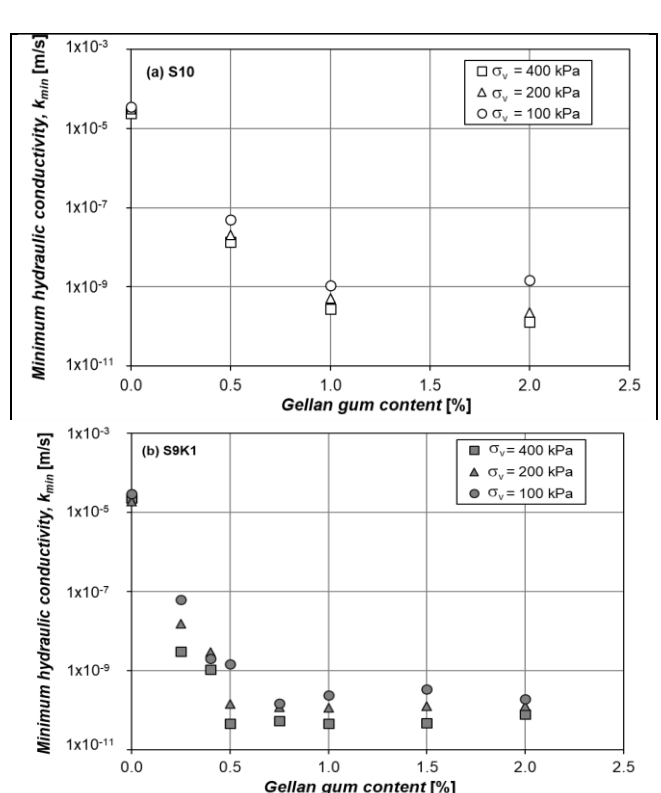


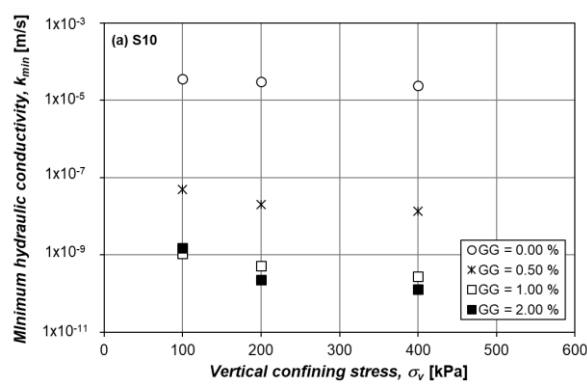
Fig. 7 Reduction in minimum hydraulic conductivity with gellan gum content of (a) 100% sand (S10) and (b) sand – kaolinite mixture S9K1

Moreover, the  $k_{min}$  values slightly decrease with higher  $\sigma_v$  (Fig. 8) which implies the denser packing of soil particles, as well as the possibility of extending the swelling time duration of GG and clays (Lejcuś *et al.* 2018). However, under the same  $\sigma_v$  conditions, the  $k_{min}$  values of the S9K1 soil were lower than the  $k_{min}$  of S10 soils (Fig. 9) which implies the effective role of GG-kaolinite matrix formation for soil hydraulic conductivity control.

#### 4. Discussions

# 4.1 Interaction mechanism of GG with pressurized inlet water

For the untreated soil, water can be drained out easily without any interruption under  $u_{in}$  higher than 70 kPa



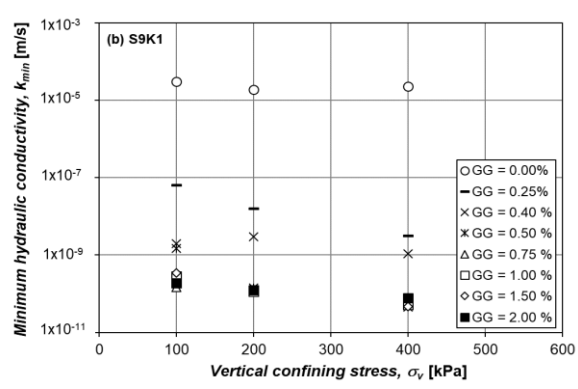


Fig. 8 Effect of vertical confining stress on minimum hydraulic conductivity of (a) 100% sand and (b) sand – kaolinite mixture

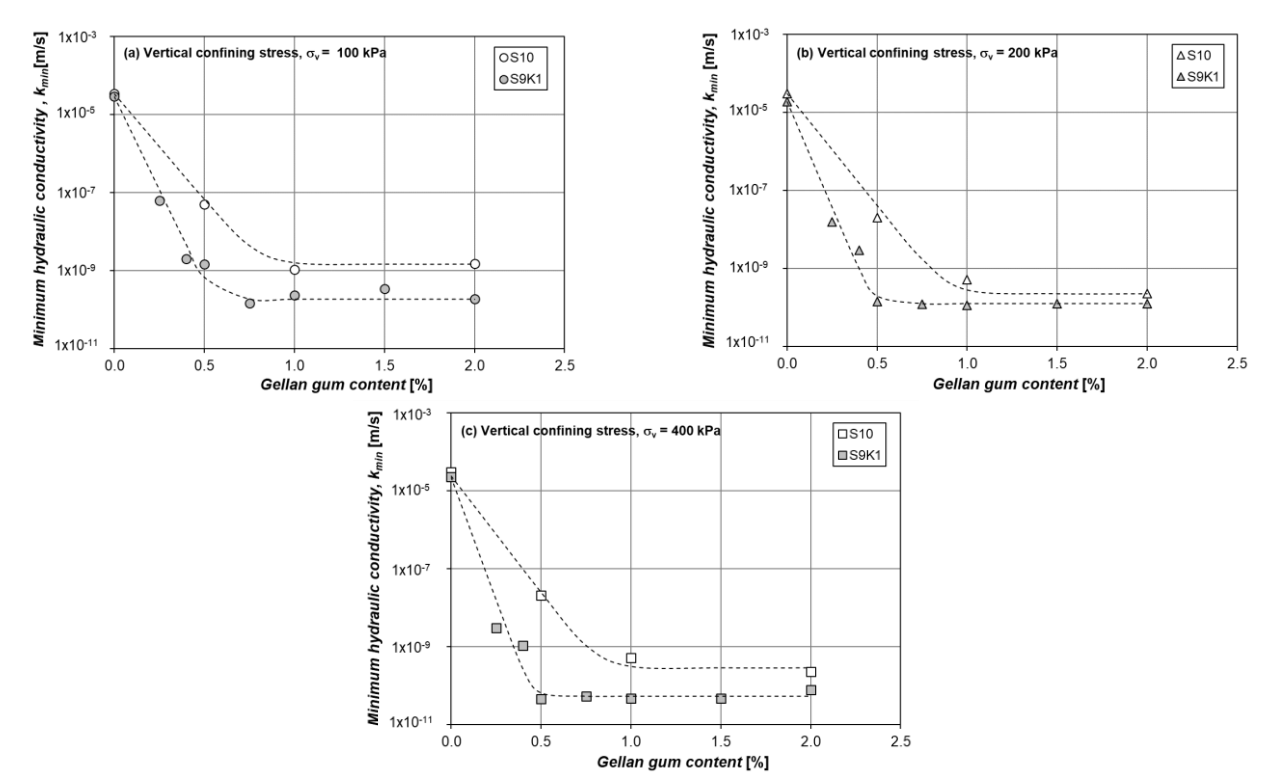


Fig. 9 Effect of clay particles on minimum hydraulic conductivity of soils under varying vertical confining stresses

because of the inconsiderable interaction forces among soil particles and soil particles – water molecules. Furthermore, the drained-out water molecules are immediately replaced by injected water molecules. Therefore, a constant in k with the  $u_{in}$  is also obtained (Figs. 3(a) and 4(a)).

For the GG-treated soil, due to the pore-clogging effect of GG hydrogel, the water flow into the soil becomes restricted (Chang *et al.* 2016). However, the water molecules continuously transport through saturated GG hydrogels via the combination of osmosis driving force due to the difference in ion concentration (Ottenbrite et al. 2010) and compression force of water flow. As a result, the water holding capacity of the soil system decreases as the water pressure higher than  $P_{k\_min}$ . Therefore, the hydraulic conductivity reaches the  $k_{min}$  at  $P_{kmin}$  and starts increasing with higher  $u_{in}$  (Figs. 3(b)-3(d) and 4(c)-4(h)).

#### 4.2 Exponential decay of hydraulic conductivity

Fig. 10 shows the  $k_{min}$  -  $c_{gg}$  relationship of S9K1 soil at  $\sigma_v = 200$  kPa, where the overall trend is attempted to be expressed as Eq. (8)

$$k_{\min} = k_0 - \alpha \left( 1 - e^{-\beta \cdot c_{gg}} \right) \tag{8}$$

where  $k_0$  presents the hydraulic conductivity of untreated  $(c_{gg} = 0\%)$  condition;  $\alpha$  becomes the inflection point of the curve;  $\beta$  is the decay parameter, which reflects the slope of the decreasing line.

The relationship between  $k_{min}$  and  $c_{gg}$  is found to show an exponential decay with  $R^2 = 0.99$  (Table 4 and Fig. 10). The  $\beta$  values of S9K1 soil are much higher than the  $\beta$  values of S10 soil (Table 4) where clay in S9K1 provides a significant role in hydraulic conductivity reduction

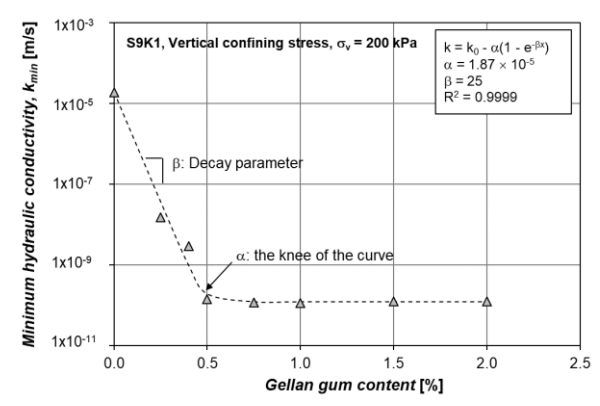


Fig. 10 An example of the trendline for minimum hydraulic conductivity of gellan gum biopolymer-treated S9K1

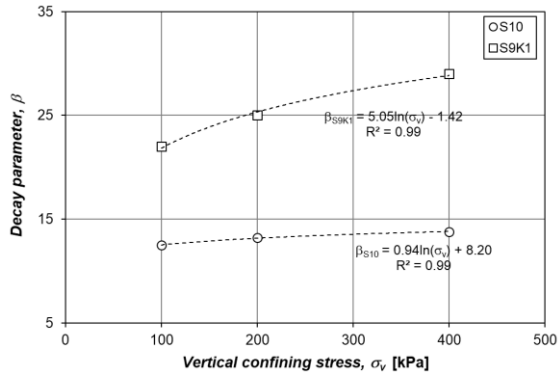


Fig. 11 Relationship between decay parameter and vertical confining stress

Table 4 Parameters for the exponential decay trendlines

Soil types	Vertical confining stress	α	β	R <sub>2</sub>
S10	100	$3.50\times10^{\text{-}5}$	12.5	1.00
	200	$3.02\times10^{-5}$	13.2	1.00
	400	$2.43 \times 10^{-5}$	13.8	1.00
S9K1	100	$4.48 \times 10^{-7}$	20.0	0.99
	200	$3.77 \times 10^{-7}$	26.0	0.99
	400	$4.49 \times 10^{-7}$	32.0	1.00

compared to S10 soil at a same  $c_{gg}$  condition. In addition, the  $\beta$  values plotted along  $\sigma_{\nu}$  (Fig. 11) show gradual increase with higher  $\sigma_{\nu}$ , where S9K1 soil shows higher dependency to  $\sigma_{\nu}$ .

The application of confinement stress reduces pore spaces within the soil matrix, thereby enhancing interactions among soil particles, between soil and gel, and among gel structures themselves. These intensified interactions promote a more effective pore-clogging mechanism by the gel. As a result, the hydraulic conductivity of the soil decreases with increasing confining stress under identical soil and treatment conditions. Here, the decay parameter  $\beta$  reflects the rate at which hydraulic conductivity declines with gel concentration. Accordingly,

an increase in the  $\beta$  parameter was observed with higher confining stress, as shown in Fig.11.

geotechnical engineering practice, improvement materials are required not only to strengthen the ground but also to control the hydraulic conductivity of soils if an adjacent water source raises instability concerns to a geotechnical engineering structure. As reported from previous studies, GG shows adequate soil strengthening and does not accompany environmental pollution which can be regarded as a new environmentally-friendly material in geotechnical engineering (Chang et al. 2016, Tran et al. 2022). In addition, results of this study show that GG BPST effectively controls the soil hydraulic conductivity under pressurized conditions, which provides an optimistic potential to use GG BPST for groundwater control practices. The effect of hydraulic conductivity reduction with  $c_{gg}$  is shown to decrease nonlinearly and level off at approximately  $c_{gg} = 1.0\%$  for S10 and  $c_{gg} = 0.5\%$  for S9K1, where those conditions can be suggested to be the most feasible GG BPST conditions for soil hydraulic conductivity control.

#### 5. Conclusions

This study demonstrates the influence of GG on the hydraulic conductivity characteristic of jumunjin sands considering in-situ stresses such as vertical confining stress  $\sigma_v$  and groundwater pressure (i.e., constant hydraulic pressure). Based on the results presented in this paper, the following conclusions are drawn:

- GG biopolymer reduces the movement of pressurized water flowing through the GG-treated soil via rendering pore-clogging effect. Affecting factors of the pore-clogging effect of GG on the soils are constant hydraulic pressure, vertical confining stress, and GG content. The hydraulic conductivity k of the untreated soils are almost constant; while for the treated soil, the k decreases to a minimum value and then turns to increase with  $u_{in}$  increase. The vertical confining pressure slightly affects the  $k_{min}$  obtained via densening the soil package.
- GG improves inter-particle bonding between sand and kaolinite particles; therefore, GG can significantly reduce the loss of fine particles under high inlet water pressure and enhance the stability of the soil system. Furthermore, the formation of GG-kaolinite matrix improves the soil hydraulic conductivity control.
- By curve fitting approximation, the relationship between the hydraulic conductivity and GG content show a good exponential decay relationship with correlation coefficients are > 0.99. Furthermore, the effect of vertical confining stress on hydraulic conductivity-GG relationship shows a logarithm trend. These relationships can become a useful tool for engineers to have a general evaluation, prediction of the hydraulic conductivity of the GG—soil treatment in the site application at where the effective stress or excess water pressure need to be considered.

In conclusion, the significant enhancement in hydraulic behavior of GG-treated soil considering in-situ stresses presents the considerable potential of GG for geotechnical engineering applications such as grouting and hydraulic barrier materials which can control the water leakage, leachate, and pressure distributions.

In this study, to investigate the role of gellan gum in hydraulic control within soils, only Jumunjin sand (S10) and a sand–kaolinite mixture (S9K1) were used. Therefore, the generalizability of the findings to soils with high plasticity is limited. Further studies are needed on soils with higher clay content and varying clay types. Further experimental investigation at GG concentration below 0.25 % would help validate and expand upon the current findings. This could be a valuable direction for future research.

#### **Acknowledgments**

The first author acknowledges the partial support of Hue University under the Core Research Program, Grant No. NCM.DHH.2018.03. Experimental study of this research was supported by the Korea Environment Industry & Technology Institute (KEITI) through Research and Development on the Technology for Securing the Water Resources Stability in Response to Future Change Program, funded by Korea Ministry of Environment (MOE) (RS-2024-00332877).

#### References

- Andry, H., Yamamoto, T., Irie, T., Moritani, S., Inoue, M. and Fujiyama, H. (2009), "Water retention, hydraulic conductivity of hydrophilic polymers in sandy soil as affected by temperature and water quality", *J. Hydrol.*, **373**(1-2), 177-183. https://doi.org/10.1016/j.jhydrol.2009.04.020.
- Bear, J. (2012), *Hydraulics of groundwater*: Courier Corporation. Bear, J. (2013), *Dynamics of fluids in porous media*: Courier Corporation.
- Chang, I. and Cho, G.C. (2019), "Shear strength behavior and parameters of microbial gellan gum-treated soils: from sand to clay", *Acta Geotechnica*, **14**, 361-375. https://doi.org/10.1007/s11440-018-0641-x.
- Chang, I., Cho, G.C. and Tran, T.P.A. (2024), "Water-retention properties of xanthan-gum-biopolymer-treated soils", *Environ. Geotech.*, 11(2), 152-163. https://doi.org/10.1680/jenge.22.00098.
- Chang, I., Im, J. and Cho, G.C. (2016), "Geotechnical engineering behaviors of gellan gum biopolymer treated sand", *Can. Geotech. J.*, **53**(10), 1658-1670. https://doi.org/10.1139/cgj-2015-0475
- Chang, I., Lee, M., Tran, A.T.P., Lee, S., Kwon, Y.M., Im, J. and Cho, G.C. (2020), "Review on biopolymer-based soil treatment (BPST) technology in geotechnical engineering practices", *Transport. Geotech.*, **24**, 100385. https://doi.org/10.1016/j.trgeo.2020.100385.
- Chang, S.H., Gupta, R.K. and Ryan, M.E. (1992), "Effect of the adsorption of polyvinyl alcohol on the rheology and stability of clay suspensions", *J. Rheology*, **36**(2), 273-287. https://doi.org/10.1122/1.550345.
- Chen, C. and Wagenet, R.J. (1992), "Simulation of water and chemicals in macropore soils Part 1. Representation of the equivalent macropore influence and its effect on soilwater flow", *J. Hydrol.*, **130**(1-4), 105-126. https://doi.org/10.1016/0022-1694(92)90106-6.

- Dumitriu, S. and Popa, V.I. (2013), *Polymeric biomaterials*, **2**, CRC Press.
- Etemadi, O., Petrisor, I.G., Kim, D., Wan, M.W. and Yen, T.F.J.S. (2003), "Stabilization of metals in subsurface by biopolymers: Laboratory drainage flow studies", *Soil Sediment Contamination*, **12**(5), 647-661. doi:https://doi.org/10.1080/714037712.
- Guilherme, M.R., Aouada, F.A., Fajardo, A.R., Martins, A.F., Paulino, A.T., Davi, M.F., Rubira, A.F. and Muniz, E.C. (2015), "Superabsorbent hydrogels based on polysaccharides for application in agriculture as soil conditioner and nutrient carrier: A review", *Eur. Polymer J.*, **72**, 365-385. doi:https://doi.org/10.1016/j.eurpolymj.2015.04.017.
- Gun'ko, V.M., Savina, I.N. and Mikhalovsky, S.V. (2017), "Properties of water bound in hydrogels", *Gels*, **3**(4), 37. https://doi.org/10.3390/gels3040037.
- Heller, H. and Keren, R. (2002), "Anionic polyacrylamide polymers effect on rheological behavior of sodium-montmorillonite suspensions", *Soil Sci. Soc. Am. J.*, **66**(1), 19-25. https://doi.org/10.2136/sssaj2002.1900.
- Kim, M. and Corapcioglu, M.Y. (2002), "Gel barrier formation in unsaturated porous media", *J. Contam. Hydrol.*, **56**(1-2), 75-98. https://doi.org/10.1016/S0169-7722(01)00204-2.
- Kwon, Y.M., Ham, S.M., Kwon, T.H., Cho, G.C. and Chang, I. (2020), "Surface-erosion behaviour of biopolymer-treated soils assessed by EFA", *Géotechnique Lett.*, **10**(2), 106-112. https://doi.org/10.1680/jgele.19.00106.
- Lejcuś, K., Śpitalniak, M. and Dąbrowska, J. (2018), "Swelling behaviour of superabsorbent polymers for soil amendment under different loads", *Polymers*, 10(3), 271.
- Milas, M., Shi, X. and Rinaudo, M. (1990), "On the physicochemical properties of gellan gum", *Biopolymers: Original Research on Biomolecules*, **30**(3-4), 451-464.
- Mulqueen, J. (2005), "The flow of water through gravels", *Irish J. Agricult.* Food Res., 83-94. https://www.jstor.org/stable/25562534.
- Narjary, B., Aggarwal, P., Singh, A., Chakraborty, D. and Singh, R. (2012), "Water availability in different soils in relation to hydrogel application", *Geoderma*, **187**, 94-101. https://doi.org/10.1016/j.geoderma.2012.03.002.
- Osmałek, T., Froelich, A. and Tasarek, S. (2014), "Application of gellan gum in pharmacy and medicine", *Int. J. Pharmaceutics*, **466**(1-2), 328-340. https://doi.org/10.1016/j.ijpharm.2014.03.038.
- Ottenbrite, R.M., Park, K. and Okano, T. (2010), "Biomedical applications of hydrogels handbook", 204.
- Paul, F., Morin, A. and Monsan, P. (1986), "Microbial polysaccharides with actual potential industrial applications", *Biotechnol. Adv.*, 4(2), 245-259. https://doi.org/10.1016/0734-9750(86)90311-3.
- Qureshi, M. U., Mahmood, Z., Farooq, Q.U., Qureshi, Q.B., Al-Handasi, H. and Chang, I. (2022), "Engineering characteristics of dune sand-fine marble waste mixtures", *Geomech. Eng.*, **28**(6), 547-557. https://doi.org/10.12989/gae.2022.28.6.547.
- Shabani, K., Bahmani, M., Fatehi, H. and Chang, I. (2022), "Improvement of the geotechnical engineering properties of dune sand using a plant-based biopolymer named serish", *Geomech. Eng.*, **29**(5), 535-548. https://doi.org/10.12989/gae.2022.29.5.535.
- Tran, T.P.A., Chang, I. and Cho, G.C. (2019), "Soil water retention and vegetation survivability improvement using microbial biopolymers in drylands", *Geomech. Eng.*, **17**(5), 475-483. https://doi.org/10.12989/gae.2019.17.5.475.
- Tran, T.P.A., Chang, I., Tran, T.N. and Cho, G.C. (2023), "Numerical modelling of slope stabilization with xathan gumtreated soil", *Vietnam J. Earth Sci.*, **45**(1), 98-110. https://doi.org/10.15625/2615-9783/17924.

- Tran, T.P.A., Cho, H., Cho, G.C., Han, J.I. and Chang, I. (2021), "Nickel (Ni2+) removal from water using gellan gum-sand mixture as a filter material", Appl. Sci., 11(17), 7884. doi:https://doi.org/10.3390/app11177884.
- Tran, T.P.A., Katsumi, T. and Tran, T.N. (2022), "Gellan gum for
- strengthening bentonite-sand slurry", *Geotech. Eng.*, **53**(3). Zhang, S., He, F., Fang, X., Zhao, X., Liu, Y., Yu, G., Zhou, Y., Feng, Y. and Li, J. (2022), "Enhancing soil aggregation and acetamiprid adsorption by ecofriendly polysaccharides hydrogel based on Ca2+-amphiphilic sodium alginate", J. Environ. Sci., 113, 55-63. https://doi.org/10.1016/j.jes.2021.05.042.